



Full paper



Engineering interfacial adhesion for high-performance lithium metal anode

Bingqing Xu^{a,b}, Zhe Liu^c, Jiangxu Li^d, Xin Huang^b, Boyu Qie^a, Tianyao Gong^a, Laiyuan Tan^a, Xiujia Yang^a, Daniel Paley^e, Martin Dontigny^f, Karim Zaghib^f, Xiangbiao Liao^g, Qian Cheng^a, Haowei Zhai^a, Xi Chen^g, Long-Qing Chen^{c,**}, Ce-Wen Nan^b, Yuan-Hua Lin^{b,***}, Yuan Yang^{a,*}

^a Program of Materials Science and Engineering, Department of Applied Physics and Applied Mathematics, Columbia University, New York, 10027, United States

^b State Key Laboratory of New Ceramics and Fine Processing, School of Materials Science and Engineering, Tsinghua University, Beijing, 100084, China

^c Department of Materials Science and Engineering, The Pennsylvania State University, University Park, State College, PA, 16802, USA

^d Shenyang National Laboratory for Materials Science, Institute of Metal Research, Chinese Academy of Sciences, School of Materials Science and Engineering, University of Science and Technology of China, 110016, Shenyang, China

^e Department of Chemistry, Columbia University, New York, 10027, United States

^f Centre of Excellence in Transportation Electrification and Energy Storage (CETEES), Hydro-Québec, 1806 Lionel-Boulet Blvd, Varennes, Qc, J3X 1S1, Canada

^g Yonghong Zhang Family Center for Advanced Materials for Energy and Environment, Department of Earth and Environmental Engineering, Columbia University, New York, 10027, United States

ARTICLE INFO

Keywords:

Lithium metal anode
Solid electrolyte interphase
Density functional theory (DFT) calculations
Phase-field simulation
Interfacial engineering

ABSTRACT

Suppressing lithium dendrites in carbonate electrolyte remains a grand challenge for high voltage lithium metal batteries. The role of adhesion between the interfacial layer and the lithium metal in controlling lithium growth is often overlooked. Here, we find that the adhesion energy significantly influences lithium dendrite growth by the phase-field simulations, and LiAl is an attractive material with strong adhesion with lithium metal by density functional theory (DFT) calculations. Then a simple solution process is developed to form conformal nanostructured LiAl interfacial layer on the lithium metal surface. With the nanostructured LiAl alloy-based interfacial layer, the Li/Li symmetric cell can be cycled stably for more than 1100 times at 5 mA/cm², 1 mAh/cm² with a low overpotential of 170 mV. For the LiNi_{1/3}Co_{1/3}Mn_{1/3}O₂/Li full cell, this interfacial layer improves the capacity retention from 59.8% to 88.7% for 120 cycles at 1 C rate, and for the LiFePO₄/Li system, the modified lithium anode also improves capacity retention from 79.5% to 99.4% after 150 cycles. This study represents a new approach to enhance the performance of lithium anode for rechargeable batteries with high voltage and high energy density.

1. Introduction

Rechargeable lithium batteries are promising energy storage systems for wide applications including portable electronics, electric vehicles and grid-level energy storage [1–4]. With the increasing demand of higher energy density, it is critical to exploring new materials with higher specific capacity. The lithium metal anode is regarded as the “Holy Grail” for rechargeable lithium batteries as it has a high theoretical capacity of 3860 mAh/g, ten times that of the commercial graphite electrode, and the lowest electrode potential (−3.04 V vs. Standard Hydrogen Electrode) [5,6]. However, lithium tends to form uncontrollable dendrites during electrochemical cycling (Fig. 1a), which

not only reduces the coulombic efficiency (CE), consumes the electrolyte, but may also cause internal shorting and cell explosion [7–12]. Hence, it is critical to realizing dendrite-free lithium deposition to render lithium electrode practical.

Various strategies have been developed to control and suppress lithium dendrites growth in the past several years, such as 3D current collector [13–15], composites with carbon materials [16–18] and alloying with metals [19], artificial solid electrolyte interphase (SEI) [19–22], and solid state electrolyte [23–28]. In studying lithium metal anode, ether electrolyte is widely used, such as 1 M LiTFSI in DOL/DME (1:1 v/v), but ether electrolyte is typically not stable with 4 V cathode, such as LiNi_xCo_yMn_{1-x-y}O₂ (NCM), which is needed to realize high

* Corresponding author.

** Corresponding author.

*** Corresponding author.

E-mail addresses: yy2664@columbia.edu, yangyuan1985@gmail.com (Y. Yang).

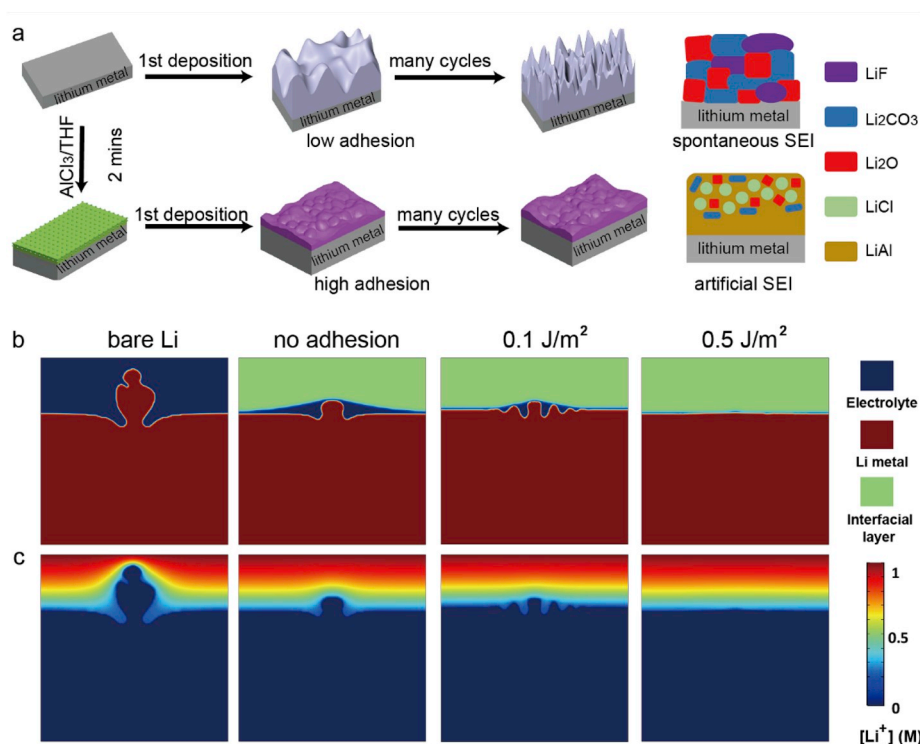


Fig. 1. (a) Lithium dendrite growth on bare lithium with a spontaneous SEI of low adhesion energy (top). Lithium dendrite suppression with a LiAl-based interfacial layer of high adhesion energy (bottom). The cartoons at the right side are SEI composition models of spontaneous SEI on lithium and AlCl₃ modified lithium. (b–c) Phase-field simulation results. The 2D phase-field simulation of Li electrodeposition at bare lithium and lithium metal anodes with coating layers of different adhesion energies: the snapshots of (b) phase morphology, and (c) Li ion concentration at $t = 1000s$. Details can be found in the section of phase-field simulations method in the supplemental information. The size for phase-field simulation is $10 \times 10 \mu\text{m}$. The applied bias between two lithium electrodes is 0.1 V.

energy density lithium batteries. On the other side, the standard LiPF₆/carbonate electrolytes are notorious for fast dendrite growth and poor CE when combined with the lithium anode [29]. Therefore, it remains a grand challenge to improve the performance of lithium metal electrode in 4 V-stable carbonate electrolytes. Interlayer design is an attractive method to suppress lithium dendrites in carbonate electrolyte, such as creating interfacial layer that has high modulus or can homogenize current distribution [21,22]. It is also a significant strategy to suppress lithium dendrites through interfacial engineering on lithium surface. Based on previous research progress, two approaches are usually adopted to construct stable and uniform SEI on lithium surface. One way is to form an artificial ex-situ SEI on Li surface in advance to guide Li⁺ deposition. The preformed SEI could be inorganic, polymeric or mixed phases, and the SEI could be single or multiple layers [30–34]. Another way is to promote homogeneous in-situ SEI formed on Li surface through rational electrolyte design [35–38]. Although Nazar group reported the synergistic effects of fast lithium ion migration from Li-rich ionic conducting alloys and insulating components [19], the adhesion between the interfacial layer and lithium has been overlooked and not investigated before.

In our work, we first demonstrate that the adhesion between the interfacial layer and lithium metal plays a significant role in suppressing lithium dendrites by phase field simulation, which shows that adhesion energy of 0.5 J/m^2 can effectively suppress dendrite growth. Then based on density functional theory (DFT) calculation, LiAl is identified as a promising candidate to achieve high adhesion energy. LiAl-rich interfacial layer is then formed by simple chemical treatment, and its effect on the electrochemical performance of batteries is tested. With such rationally designed nano-interface, stable cycling in Li/Li cells is achieved for over 400 h at 5 mA/cm^2 and 1 mAh/cm^2 , corresponding to 1000 cycles. LiFePO₄ (LFP)/Li and LiNi_{1/3}Co_{1/3}Mn_{1/3}O₂ (NCM)/Li cells also show significantly enhanced cycling performance compared to those with bare lithium anode, such as capacity retention of 99.4% vs. 79.5% for 150 cycles in LFP-Li cell at 1 C ($\sim 1.1 \text{ mA/cm}^2$), and 88.7% vs. 59.8% for 120 cycles in NCM-Li cell at 1 C ($\sim 0.93 \text{ mA/cm}^2$). These results successfully demonstrate the effectiveness of this simple AlCl₃ treatment for improving lithium anode performance in carbonate

electrolytes.

2. Material and methods

2.1. Material

LiFePO₄ powder was received from Hydro-Québec. Carbonate electrolyte (1 M LiPF₆ in ethylene carbonate (EC)/diethyl carbonate (DEC) (1:1 v/v)) was prepared without any additives. LiNi_{1/3}Co_{1/3}Mn_{1/3}O₂ (NCM) and LiCoO₂ (LCO) powder were purchased from MSE Supplies LLC and used as received. Carbon black (Super C65) was bought from Timcal. PVDF was received from Arkema. AlCl₃ powder and tetrahydrofuran (THF) were purchased from Sigma Aldrich without optimization. The separator was purchased from Celgard.

2.2. Sample preparation

The AlCl₃ powder was dissolved in THF with a concentration of 0.3 M. A lithium foil was scratched to ultra-smooth and without residual contamination. Then the lithium foil was immersed into the AlCl₃/THF solution for 2 min and taken out. Kimwipe was used to wipe the residual solutions, and the lithium foil was further washed by tetrahydrofuran (THF). The side of the lithium chip not facing separator was scratched to ultra-smooth again to remove the surface modification. The lithium foil was put into glovebox antechamber full of argon atmosphere, undergoing evacuation and refilling for five times to evaporate the residual solvents.

2.3. Battery assembly and electrochemical measurements

Li/Li cells were fabricated in carbonate electrolyte. The LiFePO₄ or LiNi_{1/3}Co_{1/3}Mn_{1/3}O₂ electrode was prepared by casting a slurry mixture onto aluminum foil containing 80 wt% LiFePO₄, LiNi_{1/3}Co_{1/3}Mn_{1/3}O₂ or LiCoO₂ powders, 10 wt% Super C65 carbon additive, and 10 wt% PVDF in 1-methyl-2-pyrrolidone (NMP). Then the aluminum foil was first dried at 80 °C for 5 h and then at 110 °C for another 2 h in the fume hood. After drying, the LiFePO₄, LiNi_{1/3}Co_{1/3}Mn_{1/3}O₂ or LiCoO₂

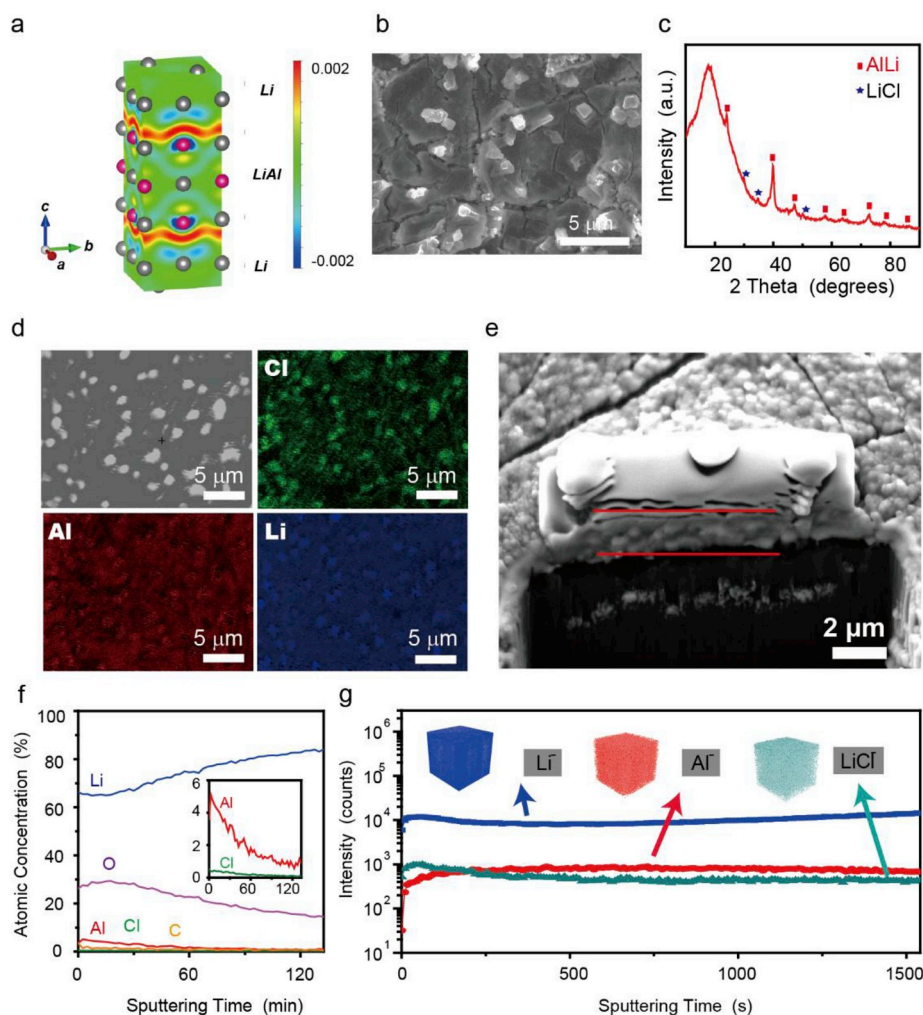


Fig. 2. (a) Charge density difference of calculated model by density functional theory (DFT). Red and blue represent high and low charge density, respectively. Color bar unit: $e/\text{\AA}^3$. Purple atoms are aluminum, and the green atoms are lithium. (b) The morphology of fresh AlCl_3 modified lithium by SEM. (c) XRD pattern of the layer after AlCl_3 reacting with Li. AlLi and LiCl peaks appear obviously. (The interfacial layer was scratched from lithium metal matrix, because the strong signals from lithium metal interfered with the XRD characterization tests.) (d) The element mapping (Cl, Al, and Li) results of AlCl_3 treated lithium by AES. (e) Cross-sectional view by FIB, the interfacial layer is about $2\ \mu\text{m}$ thick. (f) AES atomic concentration depth profile, the sputtering rate is $10\ \text{nm}/\text{min}$ based on SiO_2 . The inset picture has the same units. After 132 min, the Al and Cl signals vanishes. (g) TOF-SIMS in-depth profile of Li^+ , Al^+ , and LiCl^+ secondary ion fragments from fresh AlCl_3 treated Li. The sputtering rate is $7.5\ \text{nm}/\text{min}$. Inset pictures are the 3D views of corresponding species in the sputtered volume.

electrode was punched into disks with a diameter of 12 mm. The cells were fabricated in regular CR2032 coin cells. All the cells were assembled in a glovebox with O_2 and H_2O less than 0.5 ppm. Li/Li cells were tested in carbonate electrolyte at different current densities, 0.5, 1, 3, 5 and $10\ \text{mA}/\text{cm}^2$ with a total capacity of $1\ \text{mAh}/\text{cm}^2$. The electrochemical impedance spectroscopy (EIS) was tested by a Bio-Logic SAS VMP3 tester from 1 MHz to 0.1 Hz.

2.4. Characterizations

The microstructure images were collected from a scanning electron microscopy (SEM, MERLIN VP Compact, ZEISS). The phase structure was investigated by X-ray Diffraction (XRD, $\text{Cu K}\alpha$, D/max-V2500, Rigaku, Japan). Because the signals from lithium metal matrix was very strong, the interfacial layer was scratched and sealed in a stage with Kapton tape in glovebox with Ar atmosphere for XRD characterizations. The surface composition was analyzed by X-ray photoelectron spectroscopy (XPS, ESCALAB 250Xi electron spectrometer, Thermo Fisher Scientific), Auger electron spectroscopy (AES, PHI-700, ULVAC-PHI) and time of flight secondary ion mass spectrometry (TOF-SIMS, TOF, SIMS 5-100, ION-TOF GmbH) were used to analyze the distribution of elements at the interfacial layer. The sputtering rate of AES is $10\ \text{nm}/\text{min}$ based on SiO_2 . The sputtering rate of TOF-SIMS is $7.5\ \text{nm}/\text{min}$. The cross-sectional morphology was collected by focused ion beam (FIB) technique (crossbeam340, Zeiss).

3. Results and discussion

To understand the effect of interfacial adhesion on dendrite growth, four different scenarios are investigated by the phase field method, including bare lithium metal anode, $3\ \mu\text{m}$ -thick layers coating lithium metal anodes with adhesion energy of 0, 0.1 and $0.5\ \text{J}/\text{m}^2$, respectively (Fig. 1b). By tuning adhesion energy from 0 to $0.1\ \text{J}/\text{m}^2$, the inhomogeneity of deposited lithium is gradually reduced with increasing adhesive energy at the interface. When the adhesion energy reaches $0.5\ \text{J}/\text{m}^2$, a smooth and flat surface of the deposited lithium metal is observed, indicating that lithium dendrites can be effectively suppressed when the interfacial adhesion between the coating and lithium is strong enough. The enhanced adhesion also leads to more uniform concentration profile of Li^+ at the electrode/electrolyte interface (Fig. 1c) and current density distribution (Fig. S5). In comparison, we also simulated the electrodeposition on bare lithium metal anode without interfacial layer, where dendritic morphology appears clearly at the anode surface (Fig. 1b, most left). In general, the poor interfacial adhesion strength (typical less than $0.1\ \text{J}/\text{m}^2$, as estimated in previous work [39]) is one of the major reasons contributing to the dendrite growth at lithium metal anodes covered by conventional SEI consisting of Li_2CO_3 , LiF, Li_2O etc [6]. formed in carbonate electrolytes. Therefore, we proposed and designed a new LiAl-based interfacial layer with high adhesion energy to suppress the dendrite formation at lithium metal anodes interface.

To identify interfacial material with high adhesion, density functional theory (DFT) calculation is used to derive the interfacial energy and adhesion energy. The calculated interfacial energy of LiAl/Li is

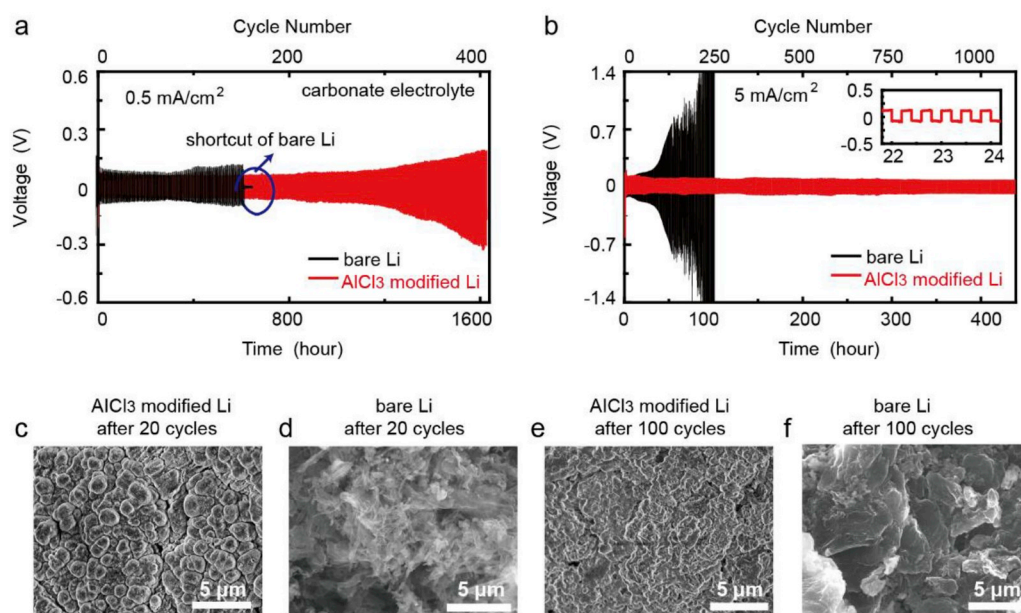


Fig. 3. (a–b) The cycling performance of Li/Li cells in carbonate electrolyte at different current densities for a total capacity of 1 mAh/cm². (a) 0.5 mA/cm². The bare Li/Li cell is shorted after 620 h, but the AlCl₃ modified Li is stable for over 1600 h. (b) 5 mA/cm². The inset picture in (b) is magnified voltage profile. More details can be found in Fig. S11. (c–f) SEM images of lithium after cycling at 1 mA/cm² and 1 mAh/cm². (c) Fresh AlCl₃ modified Li and (d) bare Li after 20 cycles. (e) Fresh AlCl₃ modified Li and (f) bare Li after 100 cycles.

–0.123 J/m², which means it is thermodynamically stable (Figs. S1–3). At the same time, Li/LiAl interface has a high adhesion energy of 1.58 J/m², representing the strong interfacial strength. Furthermore, we have calculated the charge density difference by interface model (Fig. 2a and S4), and it shows electron accumulating at the interface between LiAl and Li. This also indicates strong interfacial interactions. Due to its high stability and strong interfacial strength with lithium metal, we adopt LiAl as the interfacial layer for suppressing lithium dendrites.

The LiAl interfacial layer is realized by simply dipping a lithium foil in 0.3 M AlCl₃ in THF for 2 min followed by washing in pure THF, which is easy to scale up. Scanning electron microscopy (SEM) images illustrate that the lithium surface has nanoparticles with diameters of ~500 nm embedded in a matrix (Fig. 2b). From the X-ray diffraction (XRD) of the surface layer scratched from the lithium metal anode (Fig. 2c), the coexistence of LiCl and LiAl is further verified. In XRD, strong peaks of LiAl and weak peaks of LiCl are observed, suggesting higher portion of LiAl than LiCl. To further elucidate the spatial distribution of LiAl and LiCl, Auger electron spectroscopy (AES) mapping was carried out, showing that Cl signals formed scattered islands in a matrix of Al signals, indicating scattered LiCl domains in a matrix of LiAl (Fig. 2d). The existence of Al and Cl on the surface is also analyzed by X-ray photoelectron spectroscopy (XPS) (Fig. S8). Based on such evidence, we think the corresponding reaction is $4\text{Li} + \text{AlCl}_3 \rightarrow \text{LiAl} + 3\text{LiCl}$. Since LiCl is soluble in THF, most generated LiCl is dissolved, which left minor portion of LiCl nanodomains inside the LiAl matrix.

To further understand the composition of the interfacial layer in 3D, focused ion beam (FIB) was first employed to cut the cross section of the lithium anode, and the thickness of artificial SEI layer was estimated to be about 2 μm (Fig. 2e). Further tests by AES depth profile (Fig. 2f) and TOF-SIMS imaging (Fig. 2g) validate the existence of LiAl and LiCl through the interfacial layer, as Al and Cl were observed during the entire sputtering process. The LiAl and LiCl appear to have a higher concentration at the top (nominally ~600 nm based on a nominal sputtering rate of 10 nm/min, Fig. 2f inset), suggesting gradual transition from LiAl-based interfacial layer to the lithium metal anode. The high O content in AES may arise from the direct oxidation of Li metal and LiAl caused by the exposure of sample to air during sample transferring.

Besides morphological and compositional characterizations, the adhesion strength was also estimated by tape tests, where a kapton tape was applied to modified lithium surface and peeled off. The surface color

does not change, indicating that the interfacial layer sticks to the lithium surface very well (Fig. S9).

To investigate the effectiveness of this interfacial layer on the suppression of lithium dendrites in carbonate electrolytes, we tested the cycling stability of Li/Li cells at 0.5, 1, 3, 5 and 10 mA/cm², respectively, with a total capacity of 1 mAh/cm². All tests were performed in 1 M LiPF₆ in ethylene carbonate (EC)/diethyl carbonate (DEC) (1:1 v/v) without any additives. The modified electrodes show much better performance than bare lithium metal anode (Fig. 3a and S10a). At 0.5 mA/cm² and 1 mAh/cm², the AlCl₃ modified Li/Li symmetric cell displays a steady overpotential of 70 mV within the first 1000 h, and then gradually increases from 75 mV at the 1100th hour to 160 mV at the 1600th hour. In contrast, the bare Li/Li cell was shorted after 620 h (155 cycles). At 1 mA/cm², the AlCl₃ modified Li/Li symmetric cell delivers a stable overpotential of 80 mV for 240 h, and slightly rises to 125 mV after 360 h (Fig. S10a). Similarly, significantly better stability is also observed in AlCl₃-modified lithium anode compared to the bare lithium at 3 mA/cm² (Fig. S10b).

In previous studies, typically current density above 5 mA/cm² is unbearable in carbonate electrolytes without any additives, and the Li/Li symmetric cell either shows a very high overpotential or is shorted after a short period of cycling. In contrast, after forming nanotextured surface by AlCl₃ treatment, our cells show much more stable cycling performance at high current densities (Fig. 3b and S12). For example, at 5 mA/cm², the lithium anode is stable for over 400 h at 5 mA/cm² and 1 mAh/cm², corresponding to 1000 cycles. The overpotential is stabilized around 112 mV without further increase. Meanwhile, the overpotential of bare lithium anode increases quickly from 92 mV to 5 V within only 100 h (250 cycles), and the voltage curve fluctuates significantly (Fig. 3b). Similarly, at 10 mA/cm² and 1 mAh/cm², with the modification, the lithium anode is roughly stable for over 300 h or 1500 cycles. The overpotential is ~285 mV. Although some fluctuation is observed, it is much more stable than bare lithium anode, where the overpotential increases dramatically from 206 mV to 5 V within 50 h (Fig. S12).

The effectiveness of the interfacial layer is also demonstrated by the morphology of the lithium anode upon cycling (Fig. 3c–f). At 1 mA/cm² and 1 mAh/cm² with 1 M LiPF₆ in EC/DEC, the nanodomain-like structure still remains after 20 cycles (Fig. 3c), while the surface of bare lithium becomes mossy with fiber-like structures after 20 cycles (Fig. 3d). The difference is further amplified after 100 cycles (Fig. 3e and f). While AlCl₃ modified lithium still shows a flattened surface after 100

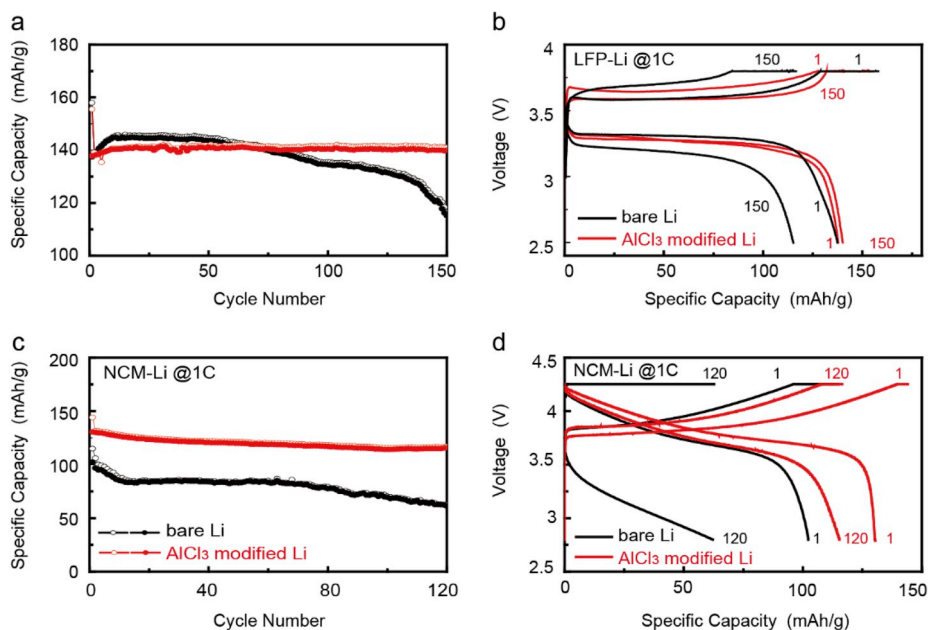


Fig. 4. Full cells performance comparison. (a–b) Cycling performance and voltage profile comparison of LFP-Li cell assembled with bare Li and AlCl₃ modified Li cycled at 1 C. The loading is 1.1 mAh/cm². (c–d) Cycling performance and voltage profile comparison of NCM-Li cell assembled with bare Li and AlCl₃ modified Li cycled at 1 C. The loading is 0.93 mAh/cm².

cycles, obvious dendrites and filament-like lithium are observed in bare lithium anode, similar to previous reports. Such results clearly show that the AlCl₃-based treatment enhances the stability of lithium anode even in carbonate electrolytes. Besides, it displays better cycling performance in ether-based electrolyte with nanostructured interface than bare Li (Fig. S13).

To further evaluate the effect of this nanostructured adhesive interfacial layer, the modified lithium anode is assembled with both LiFePO₄ (LFP) and LiNi_{1/3}Co_{1/3}Mn_{1/3}O₂ (NCM) cathode (Fig. 4). Carbonate electrolyte (1 M LiPF₆ in EC/DEC) is used in both conditions. LiFePO₄/Li (LFP-Li) cell is cycled at 1 C (Fig. 4a). While the specific capacity of LFP assembled with bare lithium is stable for the first 90 cycles, it drops fast from 136 to 115 mAh/g from cycle 90 to 150. The voltage hysteresis also increases from 309 mV at cycle 1 to 538 mV at cycle 150. In contrast, the LFP-Li cell assembled with LiAl-coated nanotextured lithium shows almost no capacity decay over the entire 150 cycles (138 mAh/g at cycle 1 to 140 mAh/g at cycle 150). In the voltage profile (Fig. 4b), the voltage hysteresis decreases from 397 mV at cycle 1 to 325 mV at cycle 150 in LFP-Li with the nanotextured LiAl-coated lithium.

Similarly, the specific capacity of a NCM-Li cell (~0.93 mAh/cm²) assembled with bare lithium decays fast from 102 mAh/g at cycle 1 to 61 mAh/g at cycle 120, when cycled between 4.25 and 3 V at 1 C, representing a capacity retention of only 59.8% (Fig. 4c). Meanwhile, the voltage hysteresis increases from 238 mV to 1.16 V from cycle 1 to cycle 120 (Fig. 4d). In contrast, with modified lithium anode, the capacity retention is improved to slow dropping from 130.4 mAh/g at cycle 1 to 115.7 mAh/g at cycle 120, showing a higher capacity retention of 88.7%. The increase in voltage hysteresis is also smaller, only from 88 mV in cycle 1 to 192 mV in cycle 120 (Fig. 4d). The coulombic efficiency (CE) of the NCM-Li cells is also improved from 98.5% with bare lithium to 98.8% with AlCl₃-modified Li (Fig. S14). We also observe that the CE is more fluctuating in bare Li than AlCl₃ modified Li, indicating poorer stability in the bare lithium anode. LiCoO₂ cathode is also assembled in full cell to test the effectiveness of nanostructured adhesive interfacial layer. It displays much enhanced cycling performance at 1C rate (Fig. S15).

Besides better cycling performance, the nanostructured surface also leads to a significant lower charge transfer impedance, which should

arise from higher surface area and probably faster reaction kinetics at the LiAl surface. In Li/Li symmetric cells, the charge transfer resistance decreases from 181 to 78 Ω after AlCl₃ treatment. Similarly, the charge transfer resistance decreases from 148 to 92 Ω in LFP-Li cell and from 144 to 62 Ω in NCM-Li cell after the AlCl₃ treatment, respectively (Fig. S16). These electrochemical data demonstrate that the nanostructures on lithium surface can help improve capacity retention in full cells with even carbonate electrolytes, which opens new opportunity to develop lithium batteries with high energy density.

4. Conclusions

In conclusion, through a combination of computation and experiments, we find that enhanced adhesion energy can help suppress the growth of lithium dendrites, and LiAl is an attractive candidate as the interfacial layer due to the strong adhesion with the lithium metal, which is calculated by density functional theory (DFT). In particular, it is shown that a LiAl-based interfacial layer can be formed on lithium metal surface by treating bare lithium metal with AlCl₃ in THF. It is demonstrated that this interfacial layer can remarkably improve the cycling stability of the Li/Li cells even in carbonate electrolyte without any additives, especially at higher current density of 5 and 10 mA/cm². The stabilized lithium with the interfacial engineered layer also leads to enhanced full cell performance with carbonate electrolytes. For example, with a LiNi_{1/3}Co_{1/3}Mn_{1/3}O₂ electrode, the capacity retention is improved from 59.8% to 88.7% at 1 C rate for 120 cycles. Such strategies can be applied to other systems with high voltage carbonate electrolytes to further increase energy density of batteries.

Declaration of competing interest

The authors declare that they have no known competing financial interests or personal relationships that could have appeared to influence the work reported in this paper.

Acknowledgments

B. X. acknowledges financial support from China Scholarship Council

(CSC) graduate scholarship. Z. L. and L.-Q.C. acknowledge the support from the Department of Energy, Office of Energy Efficiency and Renewable Energy (EERE), under the Award (DE-EE0007803). This work is also supported by Basic Science Center Project of NSFC under grant No. 51788104, and the Natural Science Foundation of China (Grant Nos. 51532003 and 51729201).

Appendix A. Supplementary data

Supplementary data to this article can be found online at <https://doi.org/10.1016/j.nanoen.2019.104242>.

References

- [1] M.S. Whittingham, Lithium batteries and cathode materials, *Chem. Rev.* 104 (2004) 4271–4302.
- [2] J. Lu, Z. Chen, Z. Ma, F. Pan, L.A. Curtiss, K. Amine, The role of nanotechnology in the development of battery materials for electric vehicles, *Nat. Nanotechnol.* 11 (2016) 1031.
- [3] B. Kang, G. Ceder, Battery materials for ultrafast charging and discharging, *Nature* 458 (2009) 190.
- [4] K. Xu, Nonaqueous liquid electrolytes for lithium-based rechargeable batteries, *Chem. Rev.* 104 (2004) 4303–4418.
- [5] P. Albertus, S. Babinec, S. Litzelman, A. Newman, Status and challenges in enabling the lithium metal electrode for high-energy and low-cost rechargeable batteries, *Nat. Energy* 3 (2018) 16–21.
- [6] X.-B. Cheng, R. Zhang, C.-Z. Zhao, Q. Zhang, Toward safe lithium metal anode in rechargeable batteries: a review, *Chem. Rev.* 117 (2017) 10403–10473.
- [7] D. Lin, Y. Liu, Y. Cui, Reviving the lithium metal anode for high-energy batteries, *Nat. Nanotechnol.* 12 (2017) 194.
- [8] Q. Cheng, L. Wei, Z. Liu, N. Ni, Z. Sang, B. Zhu, W. Xu, M. Chen, Y. Miao, L.-Q. Chen, W. Min, Y. Yang, Operando and three-dimensional visualization of anion depletion and lithium growth by stimulated Raman scattering microscopy, *Nat. Commun.* 9 (2018) 2942.
- [9] P. Bai, J. Li, F.R. Brushett, M.Z. Bazant, Transition of lithium growth mechanisms in liquid electrolytes, *Energy Environ. Sci.* 9 (2016) 3221–3229.
- [10] X.-B. Cheng, C. Yan, X.-Q. Zhang, H. Liu, Q. Zhang, Electronic and ionic channels in working interfaces of lithium metal anodes, *ACS Energy Lett.* 3 (2018) 1564–1570.
- [11] M.D. Tikekar, S. Choudhury, Z. Tu, L.A. Archer, Design principles for electrolytes and interfaces for stable lithium-metal batteries, *Nat. Energy* 1 (2016) 16114.
- [12] W. Xu, J. Wang, F. Ding, X. Chen, E. Nasybulin, Y. Zhang, J.-G. Zhang, Lithium metal anodes for rechargeable batteries, *Energy Environ. Sci.* 7 (2014) 513–537.
- [13] K. Yan, B. Sun, P. Munroe, G. Wang, Three-dimensional pie-like current collectors for dendrite-free lithium metal anodes, *Energy Storage Mater.* 11 (2018) 127–133.
- [14] H. Zhao, D. Lei, Y.-B. He, Y. Yuan, Q. Yun, B. Ni, W. Lv, B. Li, Q.-H. Yang, F. Kang, J. Lu, Compact 3D copper with uniform porous structure derived by electrochemical dealloying as dendrite-free lithium metal anode current collector, *Adv. Energy Mater.* 8 (2018), 1800266.
- [15] B. Zhu, Y. Jin, X. Hu, Q. Zheng, S. Zhang, Q. Wang, J. Zhu, Poly(dimethylsiloxane) thin film as a stable interfacial layer for high-performance lithium-metal battery anodes, *Adv. Mater.* 29 (2016), 1603755.
- [16] D. Lin, Y. Liu, Z. Liang, H.-W. Lee, J. Sun, H. Wang, K. Yan, J. Xie, Y. Cui, Layered reduced graphene oxide with nanoscale interlayer gaps as a stable host for lithium metal anodes, *Nat. Nanotechnol.* 11 (2016) 626.
- [17] L. Liu, Y.-X. Yin, J.-Y. Li, S.-H. Wang, Y.-G. Guo, L.-J. Wan, Uniform lithium nucleation/growth induced by lightweight nitrogen-doped graphitic carbon foams for high-performance lithium metal anodes, *Adv. Mater.* 30 (2018), 1706216.
- [18] G. Zheng, S.W. Lee, Z. Liang, H.-W. Lee, K. Yan, H. Yao, H. Wang, W. Li, S. Chu, Y. Cui, Interconnected hollow carbon nanospheres for stable lithium metal anodes, *Nat. Nanotechnol.* 9 (2014) 618.
- [19] X. Liang, Q. Pang, I.R. Kochetkov, M.S. Sempere, H. Huang, X. Sun, L.F. Nazar, A facile surface chemistry route to a stabilized lithium metal anode, *Nat. Energy* 2 (2017) 17119.
- [20] N.-W. Li, Y. Shi, Y.-X. Yin, X.-X. Zeng, J.-Y. Li, C.-J. Li, L.-J. Wan, R. Wen, Y.-G. Guo, A flexible solid electrolyte interphase layer for long-life lithium metal anodes, *Angew. Chem. Int. Ed.* 57 (2017) 1505–1509.
- [21] Y. Liu, Y.-K. Tzeng, D. Lin, A. Pei, H. Lu, N.A. Melosh, Z.-X. Shen, S. Chu, Y. Cui, An ultrastrong double-layer nanodiamond interface for stable lithium metal anodes, *Joule* 2 (2018) 1595–1609.
- [22] C. Yan, X.-B. Cheng, Y.-X. Yao, X. Shen, B.-Q. Li, W.-J. Li, R. Zhang, J.-Q. Huang, H. Li, Q. Zhang, An armored mixed conductor interphase on a dendrite-free lithium-metal anode, *Adv. Mater.* 30 (2018), 1804461.
- [23] F. Han, J. Yue, C. Chen, N. Zhao, X. Fan, Z. Ma, T. Gao, F. Wang, X. Guo, C. Wang, Interphase engineering enabled all-ceramic lithium battery, *Joule* 2 (2018) 497–508.
- [24] T. Dong, J. Zhang, G. Xu, J. Chai, H. Du, L. Wang, H. Wen, X. Zang, A. Du, Q. Jia, X. Zhou, G. Cui, A multifunctional polymer electrolyte enables ultra-long cycle-life in a high-voltage lithium metal battery, *Energy Environ. Sci.* 11 (2018) 1197–1203.
- [25] Q. Lu, Y.-B. He, Q. Yu, B. Li, Y.V. Kaneti, Y. Yao, F. Kang, Q.-H. Yang, Dendrite-free, high-rate, long-life lithium metal batteries with a 3D cross-linked network polymer electrolyte, *Adv. Mater.* 29 (2017), 1604460.
- [26] S. Zekoll, C. Marriner-Edwards, A.K.O. Hekselman, J. Kasemchainan, C. Kuss, D.E. J. Armstrong, D. Cai, R.J. Wallace, F.H. Richter, J.H.J. Thijssen, P.G. Bruce, Hybrid electrolytes with 3D bicontinuous ordered ceramic and polymer microchannels for all-solid-state batteries, *Energy Environ. Sci.* 11 (2018) 185–201.
- [27] P. Yao, B. Zhu, H. Zhai, X. Liao, Y. Zhu, W. Xu, Q. Cheng, C. Janyosi, Z. Li, J. Zhu, K.M. Myers, X. Chen, Y. Yang, PVDF/Palygorskite nanowire composite electrolyte for 4 V rechargeable lithium batteries with high energy density, *Nano Lett.* 18 (2018) 6113–6120.
- [28] H. Zhai, P. Xu, M. Ning, Q. Cheng, J. Mandal, Y. Yang, A flexible solid composite electrolyte with vertically aligned and connected ion-conducting nanoparticles for lithium batteries, *Nano Lett.* 17 (2017) 3182–3187.
- [29] X. Li, J. Zheng, X. Ren, M.H. Engelhard, W. Zhao, Q. Li, J.-G. Zhang, W. Xu, Dendrite-free and performance-enhanced lithium metal batteries through optimizing solvent compositions and adding combinational additives, *Adv. Energy Mater.* 8 (2018), 1703022.
- [30] Y. Gao, Z. Yan, J.L. Gray, X. He, D. Wang, T. Chen, Q. Huang, Y.C. Li, H. Wang, S. H. Kim, T.E. Mallouk, D. Wang, Polymer–inorganic solid–electrolyte interphase for stable lithium metal batteries under lean electrolyte conditions, *Nat. Mater.* 18 (2019) 384–389.
- [31] N.-W. Li, Y.-X. Yin, C.-P. Yang, Y.-G. Guo, An artificial solid electrolyte interphase layer for stable lithium metal anodes, *Adv. Mater.* 28 (2016) 1853–1858.
- [32] Y. Liu, D. Lin, P.Y. Yuen, K. Liu, J. Xie, R.H. Dauskardt, Y. Cui, An artificial solid electrolyte interphase with high Li-ion conductivity, mechanical strength, and flexibility for stable lithium metal anodes, *Adv. Mater.* 29 (2017), 1605531.
- [33] R. Xu, Y. Xiao, R. Zhang, X.-B. Cheng, C.-Z. Zhao, X.-Q. Zhang, C. Yan, Q. Zhang, J.-Q. Huang, Dual-phase single-ion pathway interfaces for robust lithium metal in working batteries, *Adv. Mater.* 31 (2019), 1808392.
- [34] C. Yan, X.-B. Cheng, Y. Tian, X. Chen, X.-Q. Zhang, W.-J. Li, J.-Q. Huang, Q. Zhang, Dual-layered film protected lithium metal anode to enable dendrite-free lithium deposition, *Adv. Mater.* 30 (2018), 1707629.
- [35] Y. Lu, Z. Tu, L.A. Archer, Stable lithium electrodeposition in liquid and nanoporous solid electrolytes, *Nat. Mater.* 13 (2014) 961.
- [36] J. Qian, W.A. Henderson, W. Xu, P. Bhattacharya, M. Engelhard, O. Borodin, J.-G. Zhang, High rate and stable cycling of lithium metal anode, *Nat. Commun.* 6 (2015) 6362.
- [37] L. Suo, W. Xue, M. Gobet, S.G. Greenbaum, C. Wang, Y. Chen, W. Yang, Y. Li, J. Li, Fluorine-donating electrolytes enable highly reversible 5-V-class Li metal batteries, *Proc. Natl. Acad. Sci.* 115 (2018) 1156.
- [38] J. Zheng, M.H. Engelhard, D. Mei, S. Jiao, B.J. Polzin, J.-G. Zhang, W. Xu, Electrolyte additive enabled fast charging and stable cycling lithium metal batteries, *Nat. Energy* 2 (2017) 17012.
- [39] Z. Liu, Y. Qi, Y.X. Lin, L. Chen, P. Lu, L.Q. Chen, Interfacial study on solid electrolyte interphase at Li metal anode: implication for Li dendrite growth, *J. Electrochem. Soc.* 163 (2016) A592–A598.



Bingqing Xu received her B.S. in Materials Chemistry from Shandong University in China in 2014. She is a Ph.D. candidate in Materials Science at School of Materials Science and Engineering at Tsinghua University in China since 2014. Now she is a visiting scholar in Department of Materials Science and Engineering at Columbia University. Her research interests focus on energy storage materials.



Zhe Liu is a PhD candidate in materials science and engineering at the Pennsylvania State University. He received his master's degree from University of Pennsylvania in 2013, and bachelor's degree from Huazhong University of Science and Technology, China in 2011, both in materials science and engineering. He interned at General Motors Warren Tech Center in 2015 and 2016 summers and worked in the Chemical and Material System Lab. He received the Jean Shollenberger Beaver Award from Pennsylvania State University in 2019, and has been an active ECS and MRS member since 2014. Zhe's research interest lies in multiscale modeling of lithium batteries coupling continuum approaches with atomic models.



Jiangxu Li received his BSc degree from the Central South University in 2015. Now, he is a PhD candidate at the Institute of Metal Research, Chinese Academy of Sciences, School of Materials Science and Engineering, University of Science and Technology of China. His research interest focuses on topological electron and topological phonon material design, topological superconductor and high throughput calculation.



Xiujia Yang has a B.S. in Materials Science from Wuhan University of Technology, Wuhan, China, and an M.S. in Materials Science from Columbia University, New York, NY. She is currently working on solid state batteries at A123 System LLC.



Xin Huang received B.Eng. in Materials Science and Engineering in Central South University, China in 2015 and M. Eng. in Materials Science and Engineering in Tsinghua University, China in 2019. Currently, he is a freelance scientific researcher. Current address: No.22 South Shaoshan Road, Changsha, China 410075.



Xiangbiao Liao is now a postdoc research scientist at Columbia Engineering. He obtained a PhD in the Department of Earth and Environmental Engineering at Columbia University in 2019, and obtained B.S. degree from University of Science & Technology of China in 2015, majoring in Theoretical and Applied Mechanics. Using multi-scale, multi-phase modeling and experimental approaches, he focuses on investigating interdisciplinary mechanics frontiers in novel materials addressing challenges in energy storage devices of flexible/structural lithium ion batteries and carbon capture/utilization.



Boyu Qie is a Ph.D. candidate in Chemistry at the University of California, Berkeley. He received his B.S in Chemistry from South University of Science and Technology of China (SUSTC) in 2015, and M.S in Material Science and Engineering from Columbia University in 2018. His research interests include exploration of synthesis and application of functional macromolecules through molecular self-assembly.



Qian Cheng received his Ph.D degree major in Materials Science and Engineering at Arizona State University in 2016. He is now a postdoctoral research scientist at Applied Physics & Applied Mathematics in Columbia University. His current research interests focus on investigating the mechanism of lithium dendrite growth on electrolytes by using stimulated Raman scattering microscopy (SRS), improving lithium-sulfur batteries in aspects of both safety and performance, and study of solid electrolyte and their protection.



Tianyao Gong received his B.S. in Materials Science and Engineering from Beihang University in China in 2017. He joined Columbia afterwards as a Master student in the Program of Materials Science and Engineering under the Department of Applied Mathematics and Applied Physics. His research is mainly focused on energy storage materials, lithium-ion batteries, solid state electrolytes, etc.



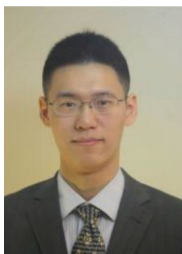
Haowei Zhai received his PhD degree (2019) from the Materials Science Program in School of Engineering and Applied Science at Columbia University, and currently he is a Postdoctoral fellow at Columbia University. His research focuses on solid electrolytes, solid-state batteries, energy materials and nanotechnology.



Laiyuan Tan obtained her B.S degree in Materials Science from University of Birmingham in UK in 2017. In the early time of this year (2019), she achieved her M.S degree in Materials Science in Columbia University.



Yuan-Hua Lin is a professor at school of materials science and engineering, Tsinghua University, Beijing, China. He was awarded as Distinguished Scholar of National Natural Science Foundation in 2010. His research interests focus on functional oxide-based ceramics and thin films, including (1) high κ ceramics and nanocomposites for high energy density capacitors applications; (2) high-temperature oxides thermoelectric materials and devices for energy conversion; (3) photoluminescence and photo-catalytic oxide nanostructured materials.



Yuan Yang is an assistant professor in the Department of Applied Physics and Applied Mathematics, Columbia University. He received his B.S. in physics from Peking University in 2007 and his Ph.D. in materials science and engineering from Stanford University in 2012. Then he worked as a postdoctoral researcher at MIT for 3 years. His research interests include electrochemical energy storage and conversion and thermal management.